

High Transverse Momentum Results from the STAR Collaboration

G. J. Kunde ^a for the STAR Collaboration and the STAR-RICH Collaboration ^{*}

^aPhysics Department, Yale University,
P.O. Box 208124, New Haven CT, 06520, USA

The STAR collaboration presents new measurements of high p_T hadron production in Au+Au and p+p collisions at RHIC. We extend the previously reported suppression of inclusive hadrons and large azimuthal anisotropies to much higher transverse momentum, decisively establishing the existence of strong medium effects on hadron production well into the perturbative regime. Near-angle two-particle correlations show directly that hadrons at $p_T > 4$ GeV/c result from the fragmentation of jets. Additional evidence for the onset of perturbative QCD in this region comes from the flavor dependence of the inclusive yields and elliptic flow. Finally, comparison of back-to-back hadron pairs at high p_T in p+p and in Au+Au collisions at various centralities reveals a striking suppression of high p_T back-to-back pairs in the most central Au+Au collisions. All of these phenomena suggest a picture in which partons or their hadronic fragments are strongly absorbed in the bulk matter, with the observed hadrons resulting from jets produced on the periphery of the collision zone and directed outwards.

1. Introduction

At energy densities larger than 1 GeV/fm³, matter is expected to undergo a phase transition from a hadronic phase to a Quark Gluon Plasma [1]. Collisions of heavy nuclei at RHIC generate an extended volume of high energy density. If this density exceeds that required for a phase transition, the evolution of the collision cannot be described purely in terms of a hadron gas and the underlying quark and gluon degrees of freedom must be invoked [2]. Hard scattering of incoming partons generates high E_T partons in the final state that propagate through the medium, eventually fragmenting into a correlated spray of hadrons called a jet. The high E_T partons interact with the surrounding medium radiating soft gluons at a rate proportional to the energy density of the medium. Measurement of jet energy loss may, therefore, provide a direct probe of the energy density [3]. This talk discusses several observables related to energy loss.

A jet may fragment in such a way that one hadron carries a large fraction of its momentum (leading hadron). The suppression of the yield of leading hadrons may signal jet energy loss. Strong suppression of high p_T hadrons has been observed in central Au+Au collisions [4,5] suggesting the existence of strong in-medium interactions, though the contribution of partonic energy loss is masked by other effects, such as shadowing and initial

^{*}For the full author list and acknowledgements see Appendix "Collaborations" in this volume.

state multiple scattering (Cronin effect) [6]. Additional evidence for strong medium effects comes from the observation of large elliptic flow in non-central collisions in which the high p_T hadron is strongly correlated with the orientation of the reaction plane of the event [7,8,9,10,11].

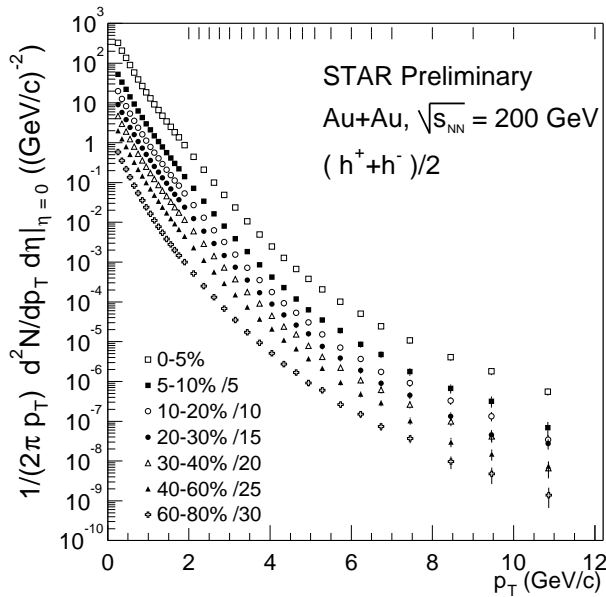


Figure 1: Invariant cross sections for charged hadrons from Au+Au collisions at $\sqrt{s_{NN}} = 200$ GeV. The hash marks indicate the bin limits.

the hadronic cross sections at high transverse momentum are dominated by pQCD processes.

The new observable, which directly probes the opacity of the medium, is the comparison of back-to-back azimuthal correlations for Au+Au and p+p. While a small suppression is observed in peripheral Au+Au collisions, central collisions are nearly devoid of back-to-back correlations. The partons or the hadrons from parton fragmentation that traverse the center of the reaction zone are either suppressed in their yield or lose the memory of their production (i.e. multiple scatter).

A large number of qualitatively new observations are presented for the first time at this conference: single inclusive spectra and v_2 to $p_T < 12$ GeV/c ; the two-particle azimuthal correlations; the precision study of non-flow contributions to high p_i ; the meson/baryon v_2 ; and identified particle ratios up to 4.5 GeV/c. A full description of the physics of high p_T hadron production must accommodate all of these phenomena.

2. Data Collection and Analysis

This paper reports the results from data taken with the STAR detector at $\sqrt{s_{NN}} = 200$ GeV during the 2001 RHIC run. The Au+Au analysis uses 2.7M minimum bias and 2.1M

Neither of the observables listed above proves experimentally that the observed hadrons are indeed the fragments of jets; for this we utilize two-particle correlations. Near-angle azimuthal two-particle correlations for Au+Au and p+p collisions are in quantitative agreement [12], indicating that hadrons with $p_T > 4$ GeV/c stem from the fragmentation of jets. This study also shows that the fragmentation of the *observed* jets is not substantially modified in Au+Au collisions. Further evidence for the onset of pQCD is the breakdown of the hydrodynamic description of the azimuthal anisotropy v_2 above $p_T > 2 - 3$ GeV/c, for both baryons and mesons. Also within the same momentum range, the measured ratio of anti-protons to protons begins to decrease with increasing momentum. All of these signatures are expected when

central triggered events (10 % of the total inelastic Au+Au cross section). Event centrality classes and numbers of participants were determined using the primary charged particle multiplicity within $|\eta| < 0.5$ [13]. The p+p data sample used in the two-particle azimuthal correlation analysis consists of 10M minimum bias events triggered by scintillator counters which cover $3.5 < |\eta| < 5.0$. Comparison is also made to the Au+Au data at $\sqrt{s_{NN}} = 130$ GeV recorded in the first year of physics running.

Charged particle tracks are measured in the TPC, which was operated in a 0.5 Tesla magnetic field. The momentum resolution is ≈ 3 % at 5 GeV/c, a factor of 3 better than in year 2000, in which the field was half the strength. Particle identification is carried out at high transverse momentum via secondary weak decays in the TPC [13] and the STAR-RICH [14] detector for primary particles at $p_T > 1.5$ GeV.

3. Results

The invariant yields for charged hadrons $(h^- + h^+)/2$ at mid-rapidity are shown in Fig. 1. The top curve represents the most central event selection, while all other centralities are scaled for clarity. The spectra are corrected for efficiency, background and momentum resolution [15]. The errors indicated include both the statistical and systematic uncertainties, and extend beyond the symbol size only at high momentum.

The onset of suppression of high transverse momentum hadrons in central collisions Au+Au was recently established in the literature [4,5], however measured in a momentum range ($p_T < 6$ GeV/c) where soft processes still contribute. It is essential that these measurements be extended to the highest possible momenta, in order to maximize the hard scattering contribution. Two related measurements have been discussed in the past:

R_{AA} , which is the ratio of AA yields to the binary collision scaled nucleon-nucleon (NN) reference, and R_{CP} , the ratio of central and peripheral yields normalized by the number of binary collisions ($\langle N_{bin} \rangle$).

At present, the NN reference is limited to $p_T < 6$ GeV/c and comes from the UA1 experiment [16]. R_{AA} at 130 GeV is reported in [5], while R_{AA} at 200 GeV gives similar results. Here we focus on the measurement which reaches farthest into the pQCD domain,

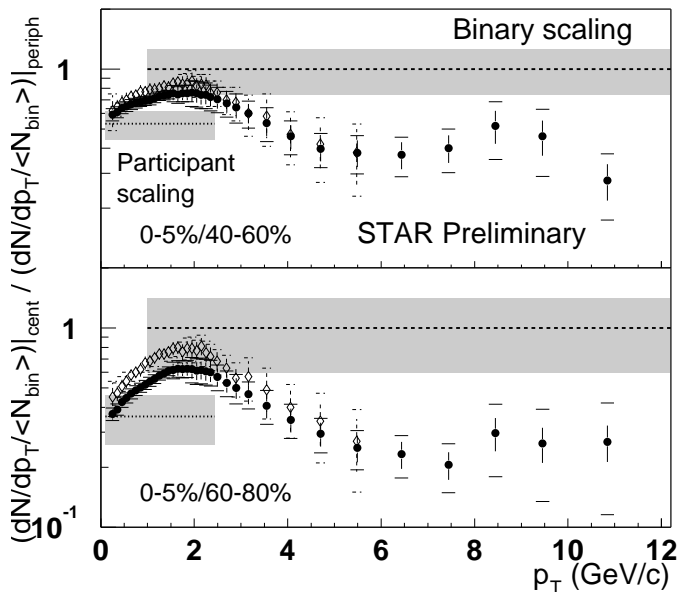


Figure 2: Ratio R_{CP} as a function of transverse momentum for central and peripheral events. The upper panel shows the ratio of the centrality classes 0-5%/40-60%, the lower panel shows 0-5%/60-80%. Error bars and bands are described in the text.

R_{CP} for $p_T < 12$ GeV/c. Calculations of the number of binary collisions $\langle N_{bin} \rangle$ and number of participants $\langle N_{part} \rangle$ are discussed in [5].

Figure 2 shows the ratio of charged hadron yields in central normalized to peripheral collisions, scaled by $\langle N_{bin} \rangle$. The 200 GeV data are represented by solid circles and the previously published 130 GeV data [5] are shown as open symbols with dashed error bars. The horizontal dashed lines and shaded areas indicate the expectations for scaling with $\langle N_{bin} \rangle$ and $\langle N_{part} \rangle$, together with their respective uncertainties.

The ratio scales approximately with $\langle N_{part} \rangle$ at low transverse momentum, and increases towards binary collision scaling at $p_T \approx 2$ GeV/c. Beyond this, the ratio decreases to $0.23\% \pm 0.06\%$ at 6.4 GeV/c for the more peripheral ratio. The qualitatively new feature of these data is the saturation of the suppression out to a p_T of 12 GeV/c. The hadron production at high transverse momentum does not follow a binary scaling but is roughly consistent with the participant scaling ([17], this proceedings). This will be discussed in more detail at the end of the paper.

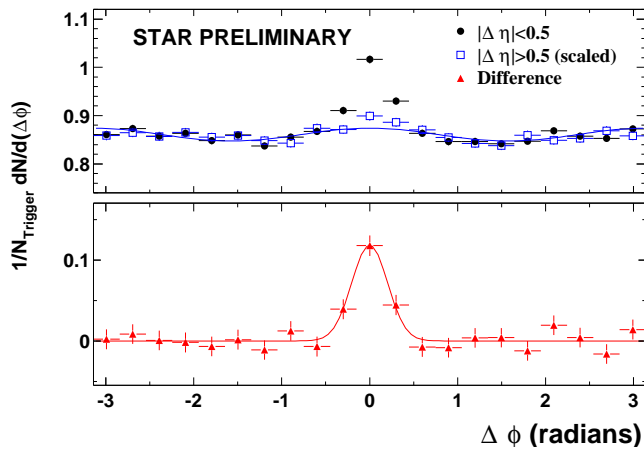


Figure 3: Azimuthal two-particle correlations for central Au+Au collisions with a trigger and associate particle for two intervals in relative pseudo-rapidity. The bottom figure shows the difference between the two measurements, suggestive of hard scattering. For details see [12].

in the range $4 < p_T < 6$ GeV/c and all associated particles in that event from $2 \text{ GeV/c} < p_T^{\text{associated}} < p_T^{\text{trigger}}$. The solid and open symbols represent the small and large pseudo-rapidity differences, respectively. The lower panel shows the difference between the two measurements which should not contain any flow effects but only near-side hard scattering and resonance contributions. (Note that due to the subtraction all back-to-back contributions cancel). The peak at small angular difference is pronounced and is suggestive of jets. Additional studies lead to the conclusion that the cross section for charged hadron production above 4 GeV/c is largely due to hard scattering processes. For a more detailed discussion see [9,12].

In a pQCD model with partonic energy loss, a strong coupling of momentum and coordinate space is predicted due to high gluon densities. This effect may be observable

In order to address directly the origin of the high p_T hadrons, we search for jet-like correlations using two-particle azimuthal correlations, see also [9]. From nucleon-nucleon collisions, it is known that the leading particles in a jet cone have a width in pseudo-rapidity of $\Delta\eta \approx 0.5$. In the Au+Au case, in addition to the jet contribution one expects azimuthal correlations due to elliptic flow, which are not localized in pseudo-rapidity. To extract the jet-specific correlations, we construct two azimuthal correlation functions of high transverse momentum particles for the relative pseudo-rapidity intervals of $\Delta\eta < 0.5$ and $\Delta\eta > 0.5$.

Figure 3 shows the two-particle correlation function for a trigger particle

in non-central collisions. Hard scattered partons undergo energy loss, whose magnitude depends on the path length of the traversed medium: initial spatial anisotropies are therefore translated into momentum anisotropies. At lower p_T , elliptic flow [7,8] dominates the measurements. The asymmetry is quantified using the observable v_2 , the second Fourier component of the azimuthal distribution of high p_T charged tracks with respect to the reaction plane. The reaction plane in turn is determined by low transverse momentum particles with $p_T < 2$ GeV/c. The detailed presentation can be found in [10] and references therein. In this paper only two highlights will be discussed, the v_2 at high transverse momentum $p_T < 12$ GeV/c and the particle-identified v_2 .

Figure 4 shows v_2 for charged hadrons as a function of the transverse momentum up to 12 GeV/c for most central events (0-10%), followed by two centrality classes (10-30% and 30-50%) and minimum-bias events. The common feature of all three centrality classes is the rising v_2 , which saturates around 2-4 GeV/c. For non-central collisions, the observed anisotropy is finite out to the highest measured transverse momentum, well into the pQCD regime. The persistence of finite anisotropy at these momenta makes the interpretation in terms of partonic or leading hadron energy loss in an asymmetric geometry rather compelling.

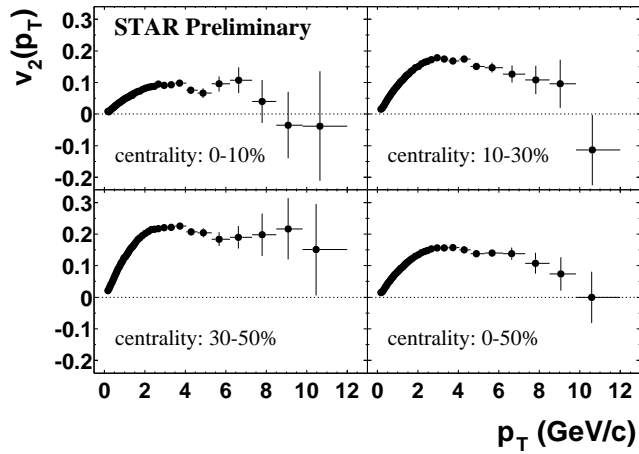


Figure 4: Azimuthal anisotropy v_2 for charged hadrons as a function of transverse momentum up to 12 GeV/c for 3 different centrality classes and for minimum-bias events. Only statistical errors are shown.

The validation of hydrodynamic calculations in predicting the elliptic flow in the soft regime lies in the particle identified measurement. At high transverse momentum, recent theoretical papers predict a different evolution of the anisotropy for mesons and baryons as a function of their transverse momentum [18,19]. Junction transport and hydrodynamics may have a large baryon cross section at intermediate p_T , while pions may be dominated by pQCD production mechanisms starting at a lower p_T .

Figure 5 shows v_2 for identified particles as a function of transverse momentum. The left panel shows pions, kaons, and (anti-)protons identified at $p_t < 1$ GeV/c via dE/dx in the TPC, while at higher p_T charged mesons and protons/anti-protons are identified track by track in the RICH detector. The right panel shows neutral kaons and lambdas identified via secondary vertices in the TPC. For all species, the low momentum behaviour of v_2 is very well described by the hydrodynamical calculations [20]. At higher momenta this prediction breaks down, baryons and mesons no longer exhaust the hydrodynamical limit; but their v_2 appears to saturate. Looking at the combined results, the heavier baryons may have a slightly higher v_2 than the mesons, though the magnitude of the difference is markedly smaller than predicted in [18].

The transverse momentum dependence of the anti-proton to proton ratio together with the anti-lambda/lambda ratio was suggested [21] as a means to study energy loss of gluons

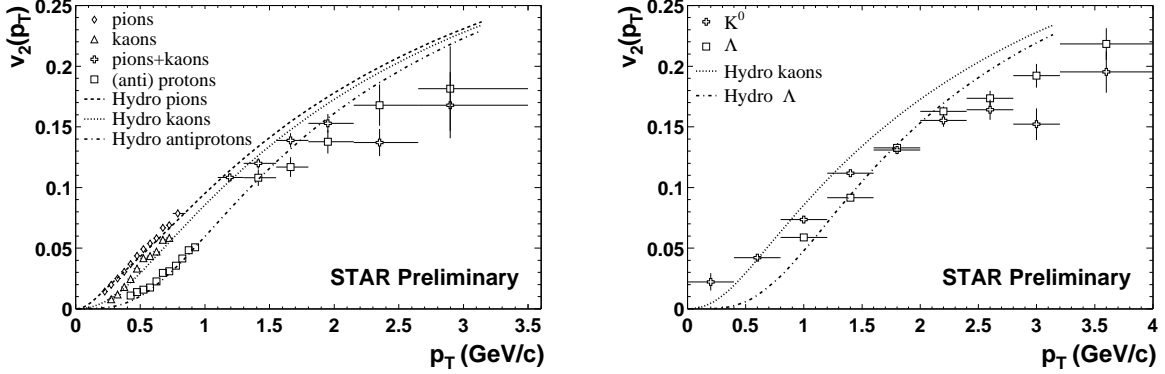


Figure 5. Azimuthal anisotropy v_2 as a function of the transverse momentum for charged mesons and baryons identified in the RICH detector (left) and neutral kaons and lambdas identified via secondary vertices in the TPC (right). Only statistical errors are shown.

versus quarks in a pQCD scenario, where the ratio is predicted to decrease with increasing p_T . However, not all observed anti-protons and protons come from fragmentation of jets. At lower transverse momenta, soft processes and possibly baryon transport play an important role. The transition from soft to hard contributions to the ratio; i.e., the transverse momentum dependence of the relative cross sections, is discussed in [22]. An observed decrease of the ratio would suggest that the transverse momentum regime at which perturbative cross sections dominate has been reached.

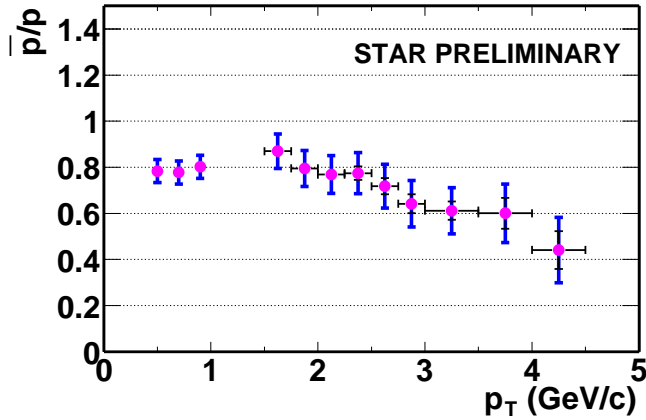


Figure 6: Anti-proton to proton ratio for 10 % central Au+Au collisions at $\sqrt{s_{NN}} = 200$ GeV as a function of transverse momentum. The low p_T particles were identified in the TPC while at the high p_T the RICH detector was used for particle identification. Statistical and systematic errors are shown.

Together with the evidence from the previous section; i.e., the breakdown of the hydrodynamic prediction for proton v_2 , this indicates pQCD dominance of the cross section in the region $p_T = 3-4$ GeV/c.

Figure 6 shows the ratio of anti-protons to protons as a function of transverse momentum for the 10% most central collisions at $\sqrt{s_{NN}} = 200$ GeV. The identification of the (anti)protons at $p_T < 1$ GeV was performed track by track via the specific energy loss dE/dx in the TPC [13]. Particle identification at high transverse momentum is obtained using a statistical analysis of the Cherenkov angle measurements with the STAR-RICH detector [14]. The ratio appears to be p_T independent up to about 2 GeV/c. This momentum independence is qualitatively in line with earlier measurements at $\sqrt{s_{NN}} = 130$ GeV [23], though the absolute ratio is larger at 200 GeV/c. The ratio decreases with increasing momentum achieving 0.44 ± 0.14 (stat + sys. errors) at 4.25 GeV/c.

Recent theoretical papers suggest the use of jets for a tomography of the medium created in Au+Au collisions. Azimuthal angular correlations of high transverse momentum track pairs were invoked earlier in this paper to indicate the existence of jets in Au+Au collisions. Here we present a new observable: back-to-back azimuthal correlations, details can be found in [12]. We summarize here the assumptions, briefly outline the procedure, and then present the results.

Because back-to-back jet correlations are not short range in η , we cannot separate elliptic flow and jet correlations in this case by studying different $\Delta\eta$ intervals. In the following, we compare Au-Au collisions with proton-proton collisions taking into account the effects of elliptic flow, which was determined independently by the reaction plane method [7,9].

In order to compare Au+Au correlation functions with the nucleon-nucleon case, a simple ansatz is suggested [12]. The correlation function $D(\text{Au+Au})$ for Au+Au is assumed to be a superposition of the correlation function $D(p+p)$ and a component describing the azimuthal anisotropy of the two particles due to the known v_2 in Au+Au collisions for the respective centrality class (see [10] and above). The explicit functional form used in the study is:

$$D^{\text{AuAu}} = D^{\text{pp}} + B(1 + 2v_2(p_T^t)v_2(p_T^a) \cos(2\Delta\phi)), \quad (1)$$

where t and a denote the trigger and associate particle, respectively. The proportionality factor B is determined by fitting the region $0.75 < |\Delta\phi| < 2.24$, which is free from jet contributions [12].

A quantitative interpretation of figure 3 is obtained by constructing the ratio I_{AA} :

$$I_{AA}(\Delta\phi_1, \Delta\phi_2) = \frac{\int_{\Delta\phi_1}^{\Delta\phi_2} d(\Delta\phi) [D^{\text{AuAu}} - B(1 + 2v_2^t v_2^a \cos(2\Delta\phi))]}{\int_{\Delta\phi_1}^{\Delta\phi_2} d(\Delta\phi) D^{\text{pp}}}. \quad (2)$$

A ratio of unity implies azimuthal two-particle correlations in Au+Au collisions are explained by a simple superposition of p+p collisions plus elliptic flow.

Figure 7 shows the ratio I_{AA} for three classes of trigger particles for near ($|\Delta\phi| < 0.75$) and back-to-back ($|\Delta\phi| > 2.24$) azimuthal regions. The near-side ratios are shown square symbols, the back-to-back ratio as round symbols, the vertical error bars indicate the statistical error, while the horizontal error bars show the systematic error obtained by

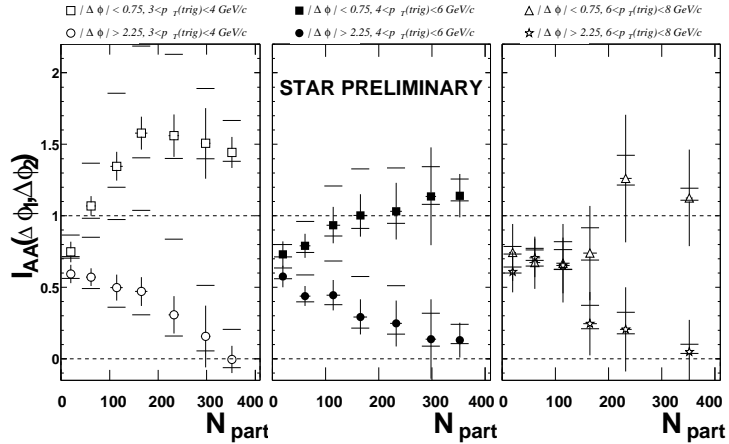


Figure 7: Ratio I_{AA} (equation 2), of Au+Au and p+p for near-side and back-to-back azimuthal regions versus number of participating nucleons. Three trigger particle thresholds $3 < p_T < 4$ GeV/c, $4 < p_T < 6$ GeV/c and $6 < p_T < 8$ GeV/c are shown in the left, middle and right panel respectively.

varying the v_2 contribution by +5-20%. The near-side ratios increase with the number of participants (centrality), while the back-to-back ratio decreases with N_{part} . In the most central Au+Au collisions, the near-side correlations are similar to those observed in p+p, while the back-to-back correlation strength is consistent with zero. The near-angle and back-to-back correlation measurements together suggest: (1) near-side jet properties are approximately unmodified by the nuclear medium, and (2) jets originate from the surface of the collision region. The disappearance of back-to-back correlations indicates strong medium effects for those jets which are either produced in the central region or propagate through the central region.

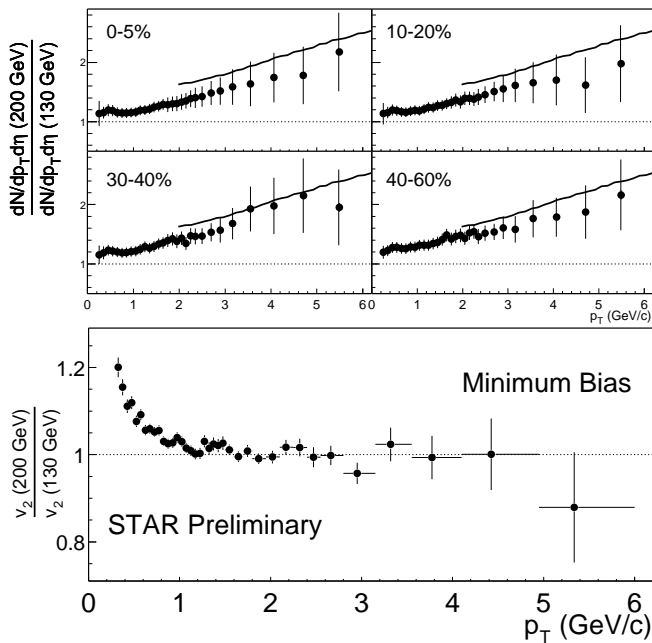


Figure 8: Upper panel: Ratio of invariant cross sections for charged hadrons as a function of transverse momentum for Au+Au collisions at $\sqrt{s_{NN}} = 200$ GeV and 130 GeV for four different centralities. The lines depict the expectations for the \sqrt{s} dependence predicted by pQCD. Lower panel: Ratio of v_2 as a function of transverse momentum for Au+Au collisions at $\sqrt{s_{NN}} = 200$ GeV and 130 GeV for minimum bias events.

the ratio is close to unity. The inclusive hadron yields grow with $\sqrt{s_{NN}}$, in line with pQCD expectations, while elliptic flow is independent of $\sqrt{s_{NN}}$. This is consistent with a surface emission picture [26], in which the origin of v_2 at high p_T is geometric and not dynamical.

The PHOBOS collaboration presented at this conference (see also [17] this proceedings) an interesting finding concerning the scaling behaviour of high p_T hadron production. Surface effects, as in the picture discussed in the previous paragraph, scale as $\langle N_{part} \rangle$. In order to study the production of high transverse momentum hadrons either $\langle N_{bin} \rangle$ or

Additional evidence for this picture is found in the \sqrt{s} dependence of hadron production and azimuthal anisotropies at high transverse momentum. The top panel of figure 8 shows the ratio of invariant cross sections as a function of p_T for Au+Au collisions at $\sqrt{s_{NN}} = 200$ GeV and 130 GeV for four different centralities. The hadron yield increases by 15-20% at low p_T for the 200 GeV data (p_T integrated yields are discussed in [13]). At a transverse momentum of 6 GeV, the hadron yield approximately doubles from 130 to 200 GeV. The solid line illustrates the \sqrt{s} dependence predicted by pQCD [25]. The ratio at high transverse momentum is within the error compatible with the pQCD predictions. No centrality dependence is observed.

The $\sqrt{s_{NN}}$ dependence of the azimuthal anisotropy $v_2(p_T)$ is shown in the lower panel of figure 8. The data for 130 GeV is taken from [9]. Elliptic flow is stronger at $\sqrt{s_{NN}} = 200$ GeV for $p_T < 1$ GeV/c, see [10]. For transverse momenta above 1 GeV/c,

$\langle N_{part} \rangle$ can be used to scale R_{AA} . The superposition of nucleon-nucleon hard scattering in the absence of nuclear effects is constructed by normalizing to the number of binary collisions. Figure 2 of this paper suggests that at high transverse momentum the data do not follow this scaling, but are closer to the N_{part} normalization.

Following the PHOBOS suggestion, we replot the STAR 130 GeV data in Figure 9. The ratio $R_{AA}^{N_{part}}$ of invariant yields measured for Au+Au collisions to the $\langle N_{part} \rangle$ scaled NN reference for 6 bins in transverse momentum is displayed as a function of the number of participants. The errors bars include both the statistical and systematic uncertainties from the Au+Au spectra and the uncertainty on $\langle N_{part} \rangle$. For the tabulated $\langle N_{part} \rangle$, see [5].

The ratios increase significantly with $\langle N_{part} \rangle$ in the 1-3 GeV/c range. A qualitatively different picture is seen in the bottom right panel, where the ratio is constant for all centralities. However, even at high pT scaling with $\langle N_{part} \rangle$ holds only within the Au+Au dataset and not with respect to the nucleon-nucleon reference.

4. Conclusion

The study of high transverse momentum hadronic probes yields several observations which must be interpreted in one consistent picture.

The experimental evidence for hard scattering lies in the fact that the two-particle azimuthal correlations for high p_T hadrons show structures which resemble jet signals, previously established for nucleon-nucleon collisions. In addition, the anti-proton to proton ratio decreases with increasing p_T , suggesting that particle production at these momenta is dominated by pQCD processes.

The suppression of high p_T hadron inclusive yields in central events with respect to the binary scaled nucleon-nucleon reference is consistent with the suppression of the back-to-back jet signal in the two-particle azimuthal correlations. This leads to the following hypothesis for central collisions: The strong absorption in the bulk matter means that those jets generated in the center of the collision zone or passing through it are strongly absorbed. The only jets that are observed are those produced near the surface, directed outwards.

While peripheral collisions appear to be a superposition of nucleon-nucleon collisions,

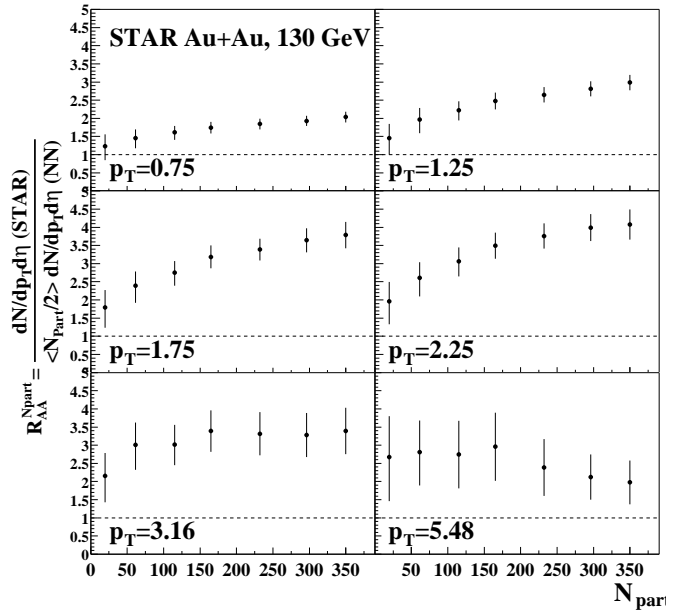


Figure 9: Ratio $R_{AA}^{N_{part}}$ of invariant cross sections in AA collisions to the $\langle N_{part} \rangle$ scaled NN reference for 6 bins in transverse momentum as a function of the number of participants (centrality). The data for 130 GeV are taken from reference [5].

this is not the case for central collisions. The question whether partonic energy loss has been clearly observed, or whether some effects can be attributed to hadron interactions with the medium, remains to be answered.

REFERENCES

1. J.W. Harris and B. Müller, Ann. Rev. Nucl. Part. Sci. **46**, 71 (1996) and references therein.
2. H.Satz these proceedings, hep-ph/0209181 (2002).
3. R.Baier, D. Schiff and B.G. Zakharov, Ann. Rev. Nucl. Part. Sci. **50**,37 (2000).
4. PHENIX Collaboration, K. Adcox, *et al.*, Phys. Rev. Lett. **88**, 022301 (2002).
5. STAR Collaboration, C. Adler *et al.*, Phys. Rev. Lett. **89**, 202301 (2002).
6. I. Vitev and M. Gyulassy, hep-ph/0209161 (2002).
7. STAR Collaboration, K. H. Ackermann *et al.*, Phys. Rev. Lett. **86**, 402 (2001).
8. STAR Collaboration, C. Adler *et al.*, Phys. Rev. Lett. **87**, 182301 (2001).
9. STAR Collaboration, C. Adler *et al.*, nucl-ex/0206006.
10. K.V. Filimonov for the STAR Collaboration, these proceedings.
11. PHENIX Collaboration, K. Adcox, *et al.*, accepted by Phys. Rev. Lett., (nucl-ex/0204005) (2002).
12. D.H. Hardtke for the STAR Collaboration, these proceedings.
13. G. Van Buren for the STAR Collaboration, these proceedings.
14. STAR-RICH and STAR Collaborations, B.Lasiuk et al., Nucl. Phys. A **698**, 452c (2002).
15. J. Klay for the STAR Collaboration, these proceedings.
16. C. Albajar, *et al.*, Nucl. Phys. **B335**, 261 (1990).
17. C. Roland for the Phobos Collaboration, these proceedings.
18. M. Gyulassy, I. Vitev, X.-N. Wang, and P. Huovinen, Phys. Lett. B **526**, 301 (2002).
19. Zi-wei Lin and C.M. Ko, nucl-th/0207014 (2002).
20. P. Huovinen et al., Phys. Lett. B **503**, 58 (2001).
21. X.N. Wang, Phys. Rev. **C58**, 2321 (1998).
22. I. Vitev and M. Gyulassy, this proceedings, hep-ph/0208108 (2002).
23. STAR and STAR-RICH Collaboration, J. Dunlop, Nucl. Phys. A **698**, 515c-518c (2002).
24. I. Vitev and M. Gyulassy, Phys. Rev. **C65**, 041902 (2002).
25. X.N. Wang, Phys. Rev. **C61**, 064910 (2000).
26. B. Müller, nucl-th/0208038, (2002).
27. E. Wang and X.N. Wang, hep-ph/0202105 (2002).
28. X.N. Wang, Phys. Rev. **C63**, 054902 (2001).